Student thesis series INES nr 299

# The Suitability of Using Landsat TM-5 Images for Estimating Chromophoric Dissolved Organic Matter in Subarctic Lakes

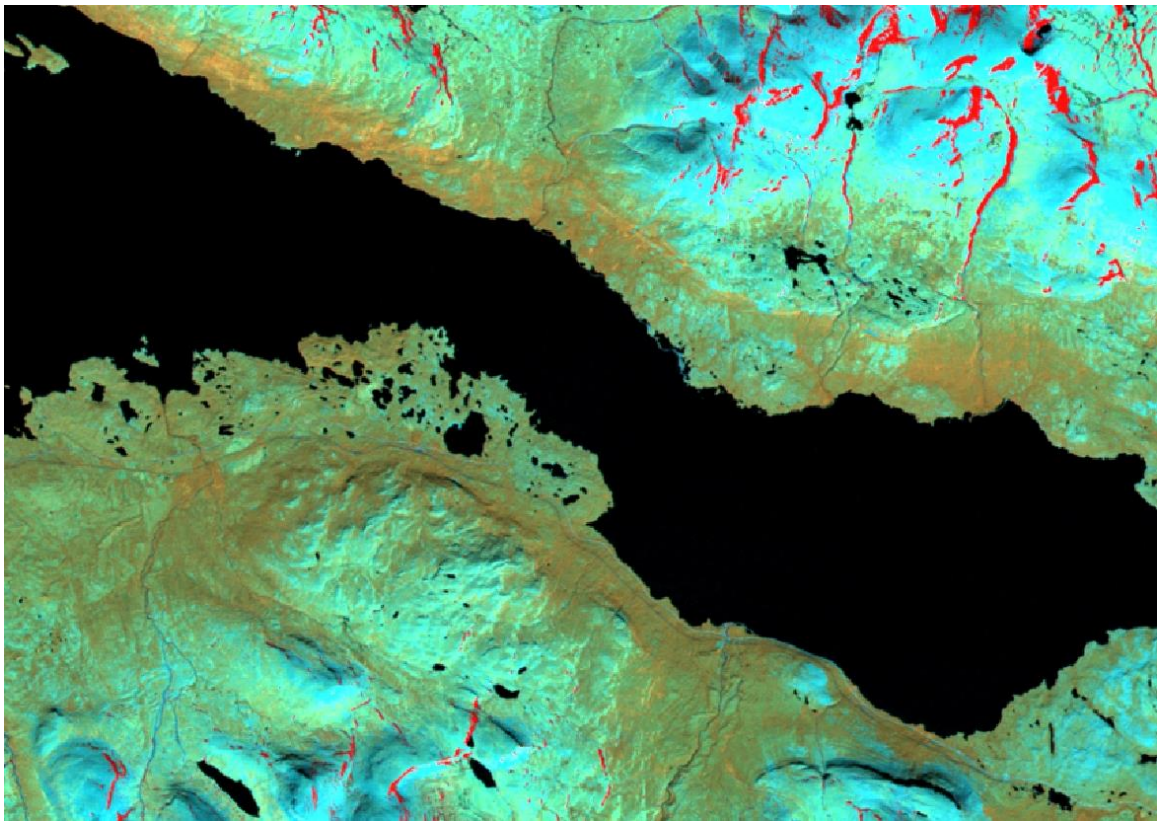

**Julia Jakobsson**

2014
Department of
Physical Geography and Ecosystems Science
Lund University
Sölvegatan 12
S-223 62 Lund
Sweden

Julia Jakobsson (2014). The suitability of Using Landsat TM-5 Images for Estimating Chromophoric Dissolved Organic Matter in Subarctic Lakes.
Bachelor degree thesis, 15 credits in *Physical Geography and Ecosystems Science*
Department of Physical Geography and Ecosystems Science, Lund University

Front page: Subset of the Landsat TM-5 2009-July-03 image displaying bands 4,5 & 6.

# The Suitability of Using Landsat TM-5 Images for Estimating Chromophoric Dissolved Organic Matter in Subarctic Lakes

**Julia Jakobsson**

Bachelor degree thesis
Physical Geography and Ecosystem Analysis
Department of Physical Geography and Ecosystems Science
January 2014

**Supervisor: Martin Berggren,**
Department of Physical Geography and Ecosystems Science
Lund University
**Technical Supervisor: Sam Kallaghi,**
Center for Geographical Information Systems
Lund University

**Acknowledgements**

Thanks to supervisor Martin Berggren for encouraging words when needed, leading with an inspirational knowledge on the subject and patient teaching. Thanks to Sam Khallaghi for not only guiding through the complexity of atmospheric corrections but excellently explaining the underlying theories of them. Thanks to Mats Eriksson at Metria for the help of finding suitable Landsat scenes and Erik Lundin at Umeå University for sharing absorbance and characteristics data from the Stordalen lakes.

**Abstract**

Recent trends of permafrost thawing in the subarctic are expected to cause increased release of dissolved organic carbon (DOC) to inland waters, which might have cascading effects on downstream aquatic ecosystems and release of $CO_2$ to the atmosphere. This study therefore aimed at evaluating the applicability of an empirical band ratio algorithm for estimating chromophoric dissolved organic matter (CDOM; a proxy for DOC) from the easily accessible satellite images Landsat TM-5, to counter the inaccessibility of the region in general. The study targeted 14 smaller lakes in the Stordalen catchment in northern Sweden where values of CDOM absorbance had been obtained from the summer of 2009 that could be used to evaluate algorithm suitability. The satellite image type and algorithm have been successfully applied to predict CDOM in previous studies of lakes with relatively high absorbance, but in this study no significant correlations were found between the in situ measured and the remote sensing estimates for the studied lakes (in situ $a_{CDOM}$ (440) = 0.29 - 1.22 $m^{-1}$; $R^2 \leq 0.21$); except for when lakes with certain characteristics were tested separately (shallow lakes $R^2 = 0.86$). It was concluded that Landsat TM-5 images are not generally suitable for estimating CDOM in the Stordalen area. However higher quality satellite products probably would; since with a higher ground-, spectral- and radiometric resolution some disturbances could be reduced, more lakes could be included in the study and they would be more accurately recorded. Nonetheless more in situ collected data is needed for supporting the discussed deductions and for adaptive algorithm modifications.

Keywords: Chromophoric, colored dissolved organic matter, CDOM, dissolved organic carbon, DOC, remote sensing, landsat thematic mapper 5, subarctic lakes, Stordalen, Abisko, empirical algorithm.

# Table of Contents

# 1. Introduction

Lakes are dynamic sites of carbon transport, transformation, and storage. It has been shown that the net carbon emissions from inland waters can be of the same magnitude as global terrestrial net ecosystem production, and that burial rates of organic carbon in freshwater sediments exceed the corresponding rates at the ocean floor (Finlay et al. 2009; Tranvik et al 2009). Inland waters therefore have environmental effects disproportionally to their spatial extent but still they are often overlooked in carbon cycling models and climate scenarios (Regnier et al., 2013).

Most carbon released to inland waters is in dissolved or particulate organic form (DOC or POC respectively) (Regnier et al., 2013). For the last decades it has been shown that concentrations of DOC in inland waters of North America and Europe have been increasing (Monteith et al., 2007). This has great impact on ecosystem functionings by stimulating organic carbon processing and emissions of $CO_2$ to the atmosphere (Lapierre et al., 2013). Increasing DOC concentrations are in part explained by decreased atmospheric anthropogenic sulfur deposition, and have recently become evident in the form of brownification of inland waters (Monteith et al., 2007; Roulet & Moore, 2006; Ekström et al., 2011).

Currently, brownification is not a major issue in subarctic waters, but certain trends gives reason to expect an upcoming change. The subarctic is estimated to store approximately 43% of the global belowground organic carbon pool in permafrost (Tarnocai et al., 2009), and as permafrost regions have been found to be warming more rapidly (Romanovsky et al. 2010) previously unavailable parts of the global soil carbon pool are made available for leaching to aquatic systems where further microbial and photochemical transformations of the carbon are likely to occur (IPCC, 2007; Tranvik et al. 1996; 2009). This is supported by findings of Laudon et al. (2012) showing that DOC concentrations are strongly related to mean annual temperatures, especially in the range of 0° to +3 °C, where regions that are currently below 0°C (mainly permafrost regions) are more likely to experience increasing concentrations of DOC than regions above (Laudon et al., 2012). However it is not only carbon derived from previously frozen soils that will be made available; as tree-limits are rising (Kullman, 2002) new organic soils will be built up and with increased terrestrially derived DOC in subarctic lakes, bacterial production and respiration is predicted to increase (Jansson et al. 2008). The changes in DOC quantity and characteristics might thus, have cascading effects on downstream aquatic ecosystems and their food webs (Berggren et al. 2009).

The monitoring of DOC in the subarctic is currently quite sporadic, considering the difficulty to access these regions, but with a functioning remote sensing protocol it would be possible to monitor changes of DOC seasonal variability and response to climate change (Kutser et al. 2005; Miller et al. 2005). One might even be able to reconstruct DOC availabilities from previous decades. Although aquatic remote sensing for inland waters have been restricted by technical obstacles there are today several satellite sensors that could possibly be utilized (Kutser et al., 2004). The reason why remote sensing has not been widely used to estimate DOC in subarctic lakes despite the availability of potential sensors today could be that DOC observation through remote sensing it is usually done by estimating the light absorbing part of dissolved organic matter, i.e., chromophoric or coloured dissolved organic matter (CDOM), and subarctic lakes are usually quite clear, thus making any variations difficult to observe. The purpose of this study is therefore to evaluate the applicability of an algorithm for CDOM estimation with satellite images that would be easily obtainable and available for time-series studies of subarctic lakes.

## 1.1. Aim

The aim of this study is therefore to test the suitability of using Landsat TM-5 images with an empirical algorithm to estimate chromophoric dissolved organic matter (CDOM). The Landsat TM-5 satellite images were chosen because of the similar spectral properties to other satellite products

that have been successfully evaluated in previous studies made by Kutser et al (2004; 2005), Kallio et al (2008) and Hirtle & Rencz (2003). Images from the Landsat archive was also chosen because of the availability of global image acquisitions since 1984 (USGS Landsat Missions, 2013a) making reconstructions of past DOC concentrations possible depending on the outcome of this study. The algorithm was also chosen based on its previous success in the studies by Kutser et al (2004; 2005) although these previous studies were performed over relatively more absorbing lakes.

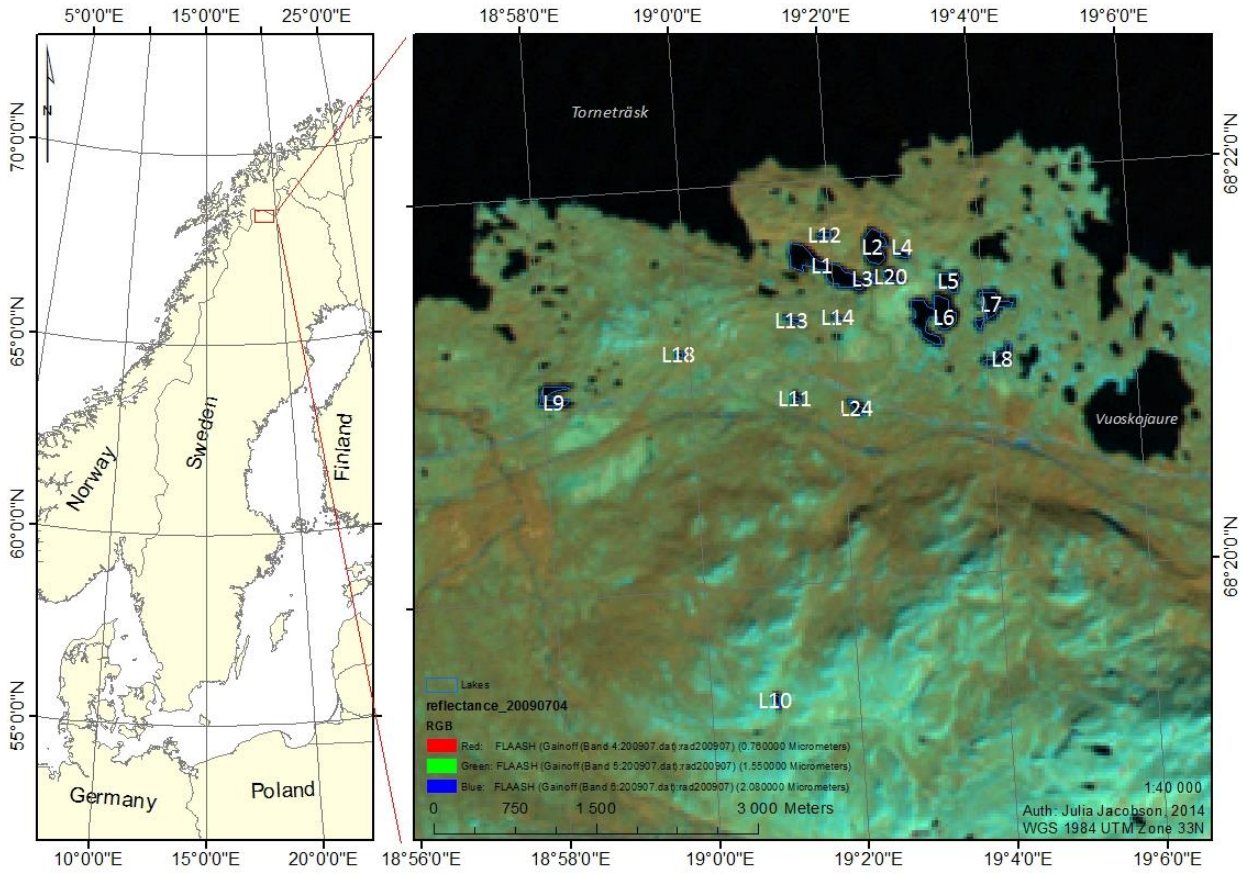


*Figure 1. Map showing the location of the study site and the locations of the lakes of interest.*

## 2. **Method**

Currently there are a number different types of algorithms developed for CDOM estimations. In this study an empirical algorithm was chosen because of successful evaluations in previous studies made by Kutser et al (2004; 2005), Kallio et al (2008) and Griffin et al (2011) for images with similar spectral properties as the ones acquired for this study. Other algorithm types available can generally be divided into four groups: semi-analytical, matrix inversion methods, spectral matching and artificial neural network (Zhu et al., 2014). However, these other algorithms are quite complex and require a lot of specific in situ data while the simpler empirical band ratio algorithm can produce just as good results (IOCCG, 2000; Zhu et al., 2014).

### 2.1. Site description

The lakes in the study are located within a peatland complex in northern Sweden in an area called Stordalen, in close vicinity of the village Abisko, just south of the lake Torneträsk (figure 1). The peatland types surrounding the lakes can be divided into fens, bogs and palsa with an

increasing shift from palsa to fen and bog (Malmer et al., 2005) due accelerating thawing trends of peatmire permafrost with a mean annual ground temperature around 0 °C (Johansson et al., 2011). The vegetation of the catchment is mainly open canopy mountain birch forest (*Betula pubescence*) with alpine heath above the tree line (Olefeldt & Roulet, 2012). Previously the vegetation surrounding the lakes have been dry shrub-dominated ombrotrophic but are now predominantly grasses in wet, nutrient rich conditions (Malmer et al., 2005; Johansson et al., 2011).

The area receives 303 mm precipitation annually (1913-2006) and has a mean annual air temperature of -0.6 °C (1913-2006) which has increased by 2.5 °C since the beginning of the measurements (Callaghan et al., 2010). The snowmelt period is 4-8 weeks which in 2009 began in early to mid-April (Olefeldt & Roulet, 2012).

Initially 27 lakes were planned to be included in the study but many had to be omitted due to their small surface sizes in relation to the ground resolution of the satellite images (30 m). In the end only 14 lakes were large enough to completely enfold at least a couple of pixels to avoid some adjacency effect of pixels close to or on shorelines.

For more specific conclusions to be drawn the lakes were classified into some grouped characteristics. Depth of the lakes were estimated and divided into 'shallow' or 'deep' on how much of the bottom could be seen in satellite images, which could be affected by water clarity. The lakes were also sorted into orders ranging from 0 to 8, where 0 means that the lake is a headwater lake, with no visible in or outflows and 8 means it is in the $8^{th}$ level of tributaries. The relative surface area classification was based on if several or few pixels could be fitted into the area but if the shape was more oblong it was still classified as small due to similar risks of adjacency effects as a smaller lake. It is also noted if the lakes have a mire upstream.

## 2.2. In situ sampling and absorption coefficients

Absorption coefficients from the lakes were received along with a short summary written by the researchers from Umeå University that had collected the data in 2009. In this summary some lake characteristics had also been noted which were used for classification purposes.

Water samples were collected in late May 2009 from the lakes in Stordalen. The samples were first filtered for 0.45 μm to remove larger particles then run through a spectrophotometer with a 5 cm cuvette. Two different types of spectrophotometers were used, with no significant differences in results. The first one was a 5-wavelength Shimandzu, the second a CIRC Jasco, recording from 200 to 900 nm.

The absorbances were initially in $cm^{-1}$ but were converted to $m^{-1}$ for correlation with the values derived from the satellite images by subtracting the 740 nm absorbance value from the 440 nm then correcting for the scale by multiplying by 100.

## 2.3. Image acquisitions

Images were obtained through the online service Saccess provided by the Swedish governmental Land Survey Department; Lantmäteriet, with help from the company Metria in finding images with the least amount of cloud cover over the area of interest. Furthermore the search was delimited by the year that the in situ absorbance water samples were collected which was in 2009. Two images were chosen from consecutive months, July and August, where the cloud cover was as minimal as possible over the target lakes.

*Table1. Wavelength specifications for Landsat TM-5.*

| Band | Wavelengths (μm) |
|---|---|
| 1 | 0.45-0.52 |
| 2 | 0.52-0.60 |
| 3 | 0.63-0.69 |
| 4 | 0.76-0.90 |
| 5 | 1.55-1.75 |
| 7 | 2.08-2.35 |

## 2.4. Atmospheric correction

For the atmospheric correction the software ENVI 5.0 was used because of the Fast Line-of-sight Atmospheric Analysis of Hypercubes (FLAASH) module which is based on the classic MODTRAN model patented by the US Air Force (Spectral Sciences Inc., 2012). The module calculates an image specific removal of aerosols and radiation back-scatter which is of great importance for aquatic remote sensing (Kutser et al 2005). Settings were adjusted according to the guides provided by Exelis VIS (2014) and used directly on the Landsat TM-5 images. In other studies such as the ones by Kutser et al (2004; 2005) the FLAASH module is applied to a Hyperion image which is then in turn used through an empirical line method to correct the main image. As Hyperion images were not available for this study that step was bypassed motivated by the fact that the images had low-to none cloud cover and very good initial visibility, and good results after visually comparing results after a so called Dark-pixel-subtraction method in the ENVI 5.0 toolkit, which is based on the empirical line principle (Smith & Milton, 1999).

To be able to perform the FLAASH correction some additional information about the imagery, satellite and location is needed, such as FWHM, Gain, Offset (table 2), units, coordinates for image center, ground elevation (380 m), ground resolution (30 m), radiometric resolution (8 bit), sensor flight height (705 km); these were found on the USGS website for Landsat 4-5TM calibration notices (USGS Landsat Missions, 2013b). Other information needed was the exact date and time of the fly-over which could be found in the metadata files belonging to the images (2009-July-03, 10:39:08 am; 2009-August-04, 10:39:09 am).

*Table 2. Landsat TM-5 FWHM, Gain and Offset used in the atmospheric correction. Due to the units of the Gain and Offset a scale factor of 10 was used to convert from $Wm^{-2}sr^{-1}\mu m^{-1}$ into $\mu W/(cm^2*sr*nm)$ (Exelis VIS, 2014).*

| Band | FWHM (μm) | Gain ($Wm^{-2}sr^{-1}\mu m^{-1}$) | Offset ($Wm^{-2}sr^{-1}\mu m^{-1}$) |
|---|---|---|---|
| 1 | 0.485 | 0.762824 | -1.52 |
| 2 | 0.560 | 1.442510 | -2.84 |
| 3 | 0.660 | 1.039880 | -1.17 |
| 4 | 0.830 | 0.872588 | -1.51 |
| 5 | 1.650 | 0.119882 | -0.37 |
| 7 | 2.215 | 0.065294 | -0.15 |

The atmospheric correction began with converting the original imagery from TIFF to ENVI format (.dat) along with subsetting the images to the area of interest. Gain and Offset values were then used to create Radiance images. To prepare the radiance images for the atmospheric correction the header files were updated with applicable values and units.

The radiance image was then used as input for the FLAASH module. Where further specifications about the satellite sensor and imagery were added such as which scale factor to use for converting the units of the radiance image and modify parameters such as atmospheric model, aerosol options and initial visibility based on prior knowledge of the area. Several combinations of options were tested but finally the atmospheric model Sub-Arctic Summer with maritime aerosol model and initial visibility >40km was decided to be the most suitable for both images.

In fairly recent studies it has also been shown that specifically Landsat images perform well, if not even better regarding water quality estimations if they are not atmospherically corrected due to the neutralizing effect of the ratio calculation (Kutser, 2012; Olmanson et al., 2008; 2011). Therefore a reference correlation with the same B2/B3 band ratio was performed for the July image. Although not for the August image as it at that stage was deemed uncontributive under the current data analysis time constraints.

## 2.5. The empirical algorithm

To extract values of absorbance a band ratio calculation was performed for Band 2 and Band 3. These bands were chosen over a Band 1 to Band 3 ratio because of the atmospheric disturbances in Band 1, due to sensor inadequacy even if CDOM absorption theoretically would affect Band 1 (0.45-0.52 μm ) more than Band 2 (0.52-0.60 μm) (Kutser et al. 2004).

A shapefile outlining the lakes of interest was used to extract the pixel values to be used for testing the model.

Two approaches to testing the extracted values were taken, one were to calculate the average of all pixels within the lake, the other were to use the most represented value within the lake, since those values varied on initial inspection. After a Shapiro-Wilk normality test in SPSS these values were then plotted for a regression model against the lake averages of the in situ measured CDOM absorbance. The power function regression is used to find the algorithm parameters which would be applied to band ratios of other images to estimate their absorption coefficients.

## 3. **Results**

In table 3 the characteristics of the selected study lakes are shown. Absorption coefficients range from 0.290 to 1.220 $m^{-1}$.

*Table 3. Lake characteristics. Lake ID with average in situ measurements of absorption coefficients from 0,5 m sample depth. Estimated lake depth from viewing satellite images. Lake order meaning how many levels of contributor lakes the lake in question have, where 0 means the lake is isolated with no visible inlets or outlets and 8 means it is the 8th lake in the flow network. Relative surface area and if the lake is downstream from a mire.*

| Lake | Average In Situ $a_{CDOM}(440)$ $m^{-1}$ | Estimated depth classification | Lake order | Relative surface area classification | Mire upstream? |
|---|---|---|---|---|---|
| L1 | 1.001 | Deep | 8 | Large | Y |
| L2 | 0.675 | Deep | 6 | Large | Y |
| L3 | 1.220 | Deep | 7 | Small | Y |
| L4 | 1.146 | Shallow | 5 | Small | Y |
| L5 | 0.594 | Shallow | 4 | Small | |
| L6 | 0.730 | Deep | 3 | Large | |
| L7 | 0.392 | Shallow | 2 | Large | |
| L8 | 0.930 | Shallow | 1 | Small | |
| L9 | 0.290 | Shallow | 1 | Small | |
| L13 | 0.992 | Deep | 1 | Small | |
| L14 | 0.646 | Shallow | 1 | Small | |
| L18 | 0.910 | Deep | 0 | Small | |
| L20 | 0.783 | Deep | 1 | Small | |
| L24 | 0.950 | Shallow | 1 | Small | |

Regression models for atmospherically corrected B2/B3 band ratios from 2009-July-03 and 2009-August-04, failed to correlate to be able to predict the average values of in situ $a_{CDOM}(440)$ absorption coefficient when all selected study lakes were analyzed together (Figure 2). Differentiating between using the most represented pixel values or the average pixel values did not change the levels of correlation either, as an $R^2$ value of at least 0.28 would be needed for 14 values to show significance (table 4).

*Table 4. Overview of images with values used and corresponding algorithms and $R^2$. It is also noted if the image was atmospherically corrected before. (APV = average pixel value, MRPV = most represented pixel value).*

| Image | Values | Algorithm | $R^2$ | Atmospheric correction |
|---|---|---|---|---|
| 2009-July-03 | APV | $A_{CDOM}(440) = 0.986(B2/B3)^{-1.094}$ | 0.192 | Yes |
| 2009-July-03 | MRPV | $A_{CDOM}(440) = 1.063(B2/B3)^{-1.231}$ | 0.214 | Yes |
| 2009-August-04 | APV | $A_{CDOM}(440) = 0.813(B2/B3)^{-0.288}$ | 0.055 | Yes |
| 2009-August-04 | MRPV | $A_{CDOM}(440) = 0.832(B2/B3)^{-0.323}$ | 0.026 | Yes |
| 2009-July-03 | APV | $A_{CDOM}(440) = 1.437(B2/B3)^{-2.656}$ | 0.092 | No |

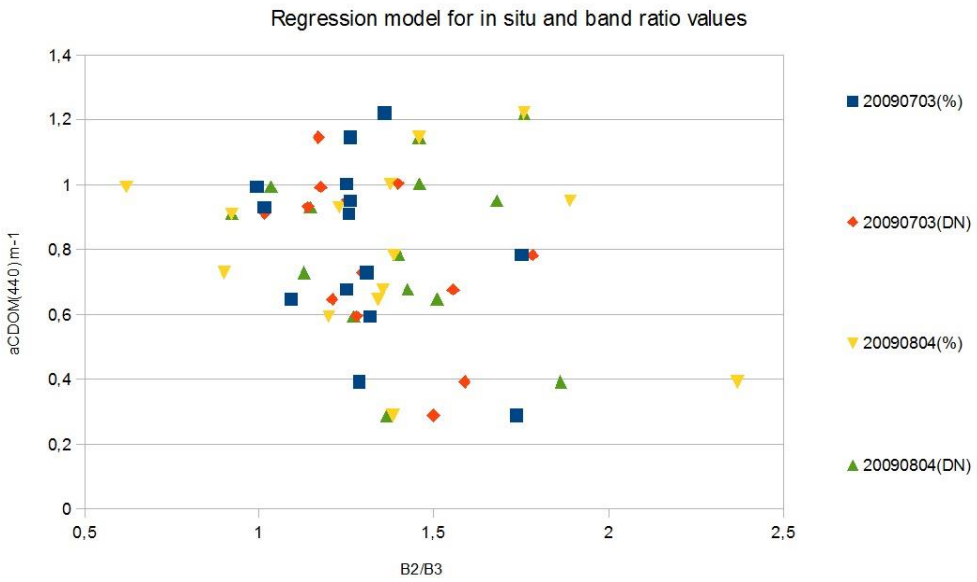


*Figure 2. In situ measurements of CDOM absorbance, $a_{CDOM}(440)$, plotted against band ratios B2/B3 from atmospherically corrected Landsat TM-5 imagery from July and August 2009.Different types of symbols show different pixel value selection types: (%) = most represented pixel value,(DN) = average pixel value. No significant correlation was found.*

All values for both 2009-July-03 and 2009-August-04 atmospherically corrected imagery B2/B3 band ratios were tested for Pearson correlation against each other which returned significant on a 2-tailed 0,001 level and were therefore combined for a clearer regression model, or a pseudo-time series, although no stronger correlation was found for either the most represented pixel values ($R^2$ = 0.082) or average pixel values ($R^2$ = 0.082)(figure 3).

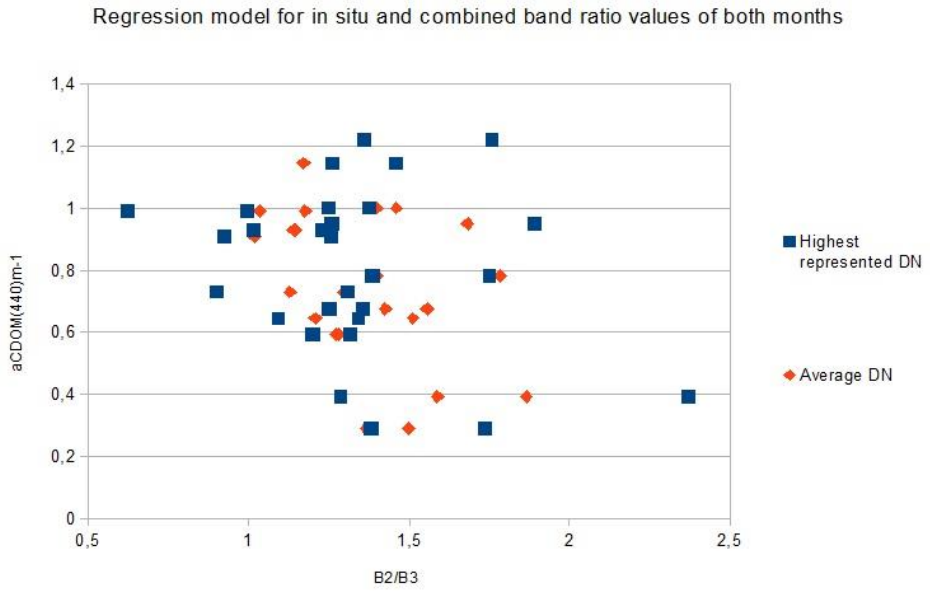


*Figure 3. In situ measurements of CDOM absorbance, $a_{CDOM}(440)$, plotted against combined band ratios B2/B3 from atmospherically corrected Landsat TM-5 imagery from July and August 2009. (MRPV = most represented pixel value, APV = average pixel value)*

The regression test for the non-atmospherically corrected image for 2009-07-03 band ratios B2/B3 with average pixel values against average values of in situ measurements of $a_{CDOM}(440)$ gave no strong correlation either ( $R^2 = 0.092$) but when the 7 lakes that had been classified as 'Shallow' in table 3 were plotted separately stronger correlations were found (figure 4 and table 5). The lakes that had been classified as 'Deep' still had no correlation ($R^2 = 0.154$) but the average pixel values for 'Shallow' lakes returned $R^2 = 0.722$ for the non-atmospherically corrected July 2009 B2/B3 ratio and $R^2 = 0.861$ for the atmospherically corrected July 2009 B2/B3 ratio. The same level of correlation was not found for the August 2009 images or for 'small/large' surface area classifications.

*Table 5. Overview of the specifications for the correlations shown in figure 4. Alla values based on average pixel values.*

| Image | Atmospheric correction | Classification | Algorithm | $A_{CDOM}(420)\ m^{-1}$ | $R^2$ | N |
|---|---|---|---|---|---|---|
| 2009-July-03 | No | Deep | $A_{CDOM}(440) = 1.18(B2/B3)^{-1.260}$ | 0.646 – 1.140 | 0.15 | 7 |
| 2009-July-03 | No | Shallow | $A_{CDOM}(440) = 9.744(B2/B3)^{-1.272}$ | 0.252 – 0.937 | 0.72 | 7 |
| 2009-July-03 | Yes | Shallow | $A_{CDOM}(440) = 1.460(B2/B3)^{-3.588}$ | 0.252 – 0.937 | 0.86 | 7 |

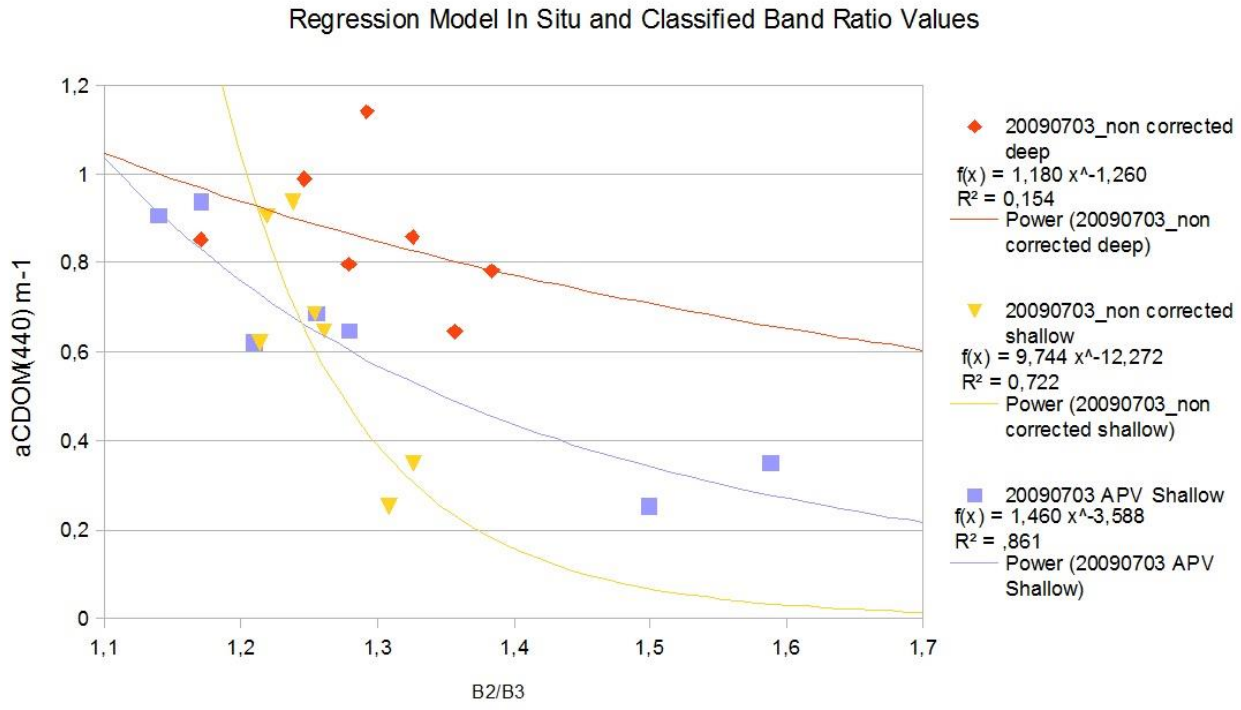


*Figure 4. Correlation between in situ measurements of CDOM absorbance, $a_{CDOM}(440)$, and band ratios B2/B3 from the non-corrected Landsat TM-5 image from July 2009 with average pixel values and divided into deep/shallow characteristics. The shallow values for the atmospherically corrected July 2009 image is also plotted.*

## 4. **Discussion**

The results gave no strong correlation between in situ measured absorption values for CDOM and the estimations from the Landsat TM-5 images. Much of the reason for this seems to be of the same nature as for a similar study made by Kutser (2012) where "the possibility of using the Landsat image archive for monitoring long time trends in colored dissolved organic matter concentration in lake waters" was studied. The Landsat sensors were found to be unfit for those purposes. The reasons for this was mainly three points according to Kutser (2012); (1) a too low radiometric resolution of only 8 bit, (2) the lake sizes being too small thus leading to large adjacency effects, which is also mentioned by Hirtle and Rencz (2003) in their use of Landsat images to measure DOC in Nova Scotian lakes. The third (3) reason according to Kutser (2012) was the high concentration of CDOM which does not seem applicable in this case, due to the relatively low absorption values from the in situ measurements.

### 4.1. Radiometric and ground resolution

The radiometric resolution of a satellite sensor determines how detailed the observed measurements can be recorded and allocated a value on a discrete radiometric interval (Miller, 2005). For example: 4 bit resolution means values from 0 to 15 is available, 8 bit resolution means values from 0 to 255 is available and 16 bit gives values from 0 to 65 536 (ESRI, 2014). These differences can be considered by visualizing the possibility of detail for a picture drawn with 15 different colours compared to one with 65 536 different colours. In this case an unsatisfactory radiometric resolution would lead to either more congregated or sharply diverse pixel values, which could be seen in the histograms of the extracted lakes, thus affecting the distribution of values which eventually is displayed by the difference between the most represented pixel value and the average pixel value. As can be seen in Figure 2 and 3 there is a slight difference between APV and MRPV values but not quite enough for it to be the sole reason for the inadequacy of the Landsat images.

It is also likely that the results are affected by spatial inadequacies leading to predominance of adjacency effects. Adjacency effects mean that reflectances from nearby objects influence one another through scattering, creating a blurring or leaking effect to reflectance values, which is especially true for lakes with small surface sizes (Tanré, 1987). To counteract adjacency effect Hirtle and Rencz (2003) selected pixel values towards the center of their lake. That was not applicable in this study as the spatial extent of the lake surfaces compared to the ground resolution of the images (30 m) was too small. Most of the lakes didn't fit many pixels to begin with and the two lakes it might be applicable to select only a few pixels from are not enough to draw a valid correlation from. In that case a longer time-series study would have to be done. Kutser (2012) found that Landsat images might be used for rough estimations of CDOM changes over time for a lake with an area of about 1140 $km^2$ which is quite a lot larger than the lakes in this study; therefore such a study would be risky but interesting for application to the subarctic lakes.

### 4.2. Atmospheric corrections

Another reason for the weak correlation could be argued to be the atmospheric correction, which possibly could reduce some of the adjacency effects, but since the $R^2$ (=0.092) value of the atmospherically uncorrected image was of the same scale, or sometimes better, than the atmospherically corrected images (table 4) it does not appear to be the main issue with the Landsat TM-5 images. The results that Landsat images perform better when not atmospherically corrected have also been found by Kutser (2012), Kallio (2008), Hirtle & Rencz (2003) and Olmanson et al. (2008; 2011); which is explained by uneven reduction of values between the bands, that become

enhanced through ratio calculations. This was also found during test corrections of the images in this study, when trying to find the most suitable settings in the FLAASH module, where some settings produced large amounts of negative pixel values, thus explained by over-correction.

## 4.3. Algorithms

Fallacies in the method of only using the simple empirical ratio algorithm could also be argued. Landsat TM images have been successfully used by Hirtle and Rencz (2003) and Griffin et al. (2011) with more complicated empirical algorithms (table 6). Although the images used by Griffin et al (2011) were mainly of the Landsat ETM+ type which has overall better resolutions than the TM-5 and the Kolyma River also have a larger spatial surface than the lakes used in this study thus enabling more selectiveness in pixel values. To develop their algorithm, a more time-series like approach was employed. That method could be applied here but better results would probably be yielded if more bands were included in the algorithm.

*Table 6. An overview of Sensors, algorithms, in situ data ranges (DOC & CDOM), correlation and numbers of samples from different studies.*

| Author (year) | Sensor | Algorithm | DOC concentration (mg $L^{-1}$) | $A_{CDOM}$ (420) $m^{-1}$ | $R^2$ | N Samples |
|---|---|---|---|---|---|---|
| Kutser et al. (2004) | ALI | $A_{CDOM}(420)=5.13(B2/B3)^{-2.67}$ | - | 0.68 – 11.13 | 0.83 | 22 |
| Kutser et al. (2005) | ALI | $A_{CDOM}(420)=5.20(B2/B3)^{-2.76}$ | 7.2 – 12.3 | 1.28 – 7.74 | 0.84 | 245 |
| Kutser et al (2012) | Landsat | - | - | 0,03 – 20,2 | - | 19 |
| Kallio et al (2008) | Landsat ETM+ | $A_{CDOM}(400) = 23.33exp(-0.970(B2/B3))$ | - | 1.0 – 12.2 | 0.83 | 29 |
| Hirtle & Rencz (2003) | Landsat TM | Log(DOC) = 3,49-0,121(B2)+0,072(B4) | 2.8 – 13.1 | - | 0.72 | 18 |
| Griffin et al. (2011) | Landsat ETM+ & TM | $a_{CDOM}(420) = exp(-1.145+26.529(B3)+0.603(B2/B1)$ | 2.14 – 9.52 | 1.38 – 6.45 | 0.78 | 18 |

## 4.4. Lake characteristics

A significant correlation to the in situ CDOM absorption was found for lakes that had been classified as shallow, but not for any other of the characteristics such as 'deep', 'small', 'large', with a mire upstream or the lake order. It does therefore not seem as just an overall level of characteristic homogeneity that determines correlation but more specifically relates to depth; unless there is just a lack of data for other correlations.

Since the waters have such low CDOM absorption values it is quite likely that the bottom substrate is influencing reflection values. In this case the difference between a vegetated bottom and a rock bottom could affect both the optical classification of depth and band values. Where vegetation might affect band 3 but rock would not be apparent until in band 6 or 7; only rock bottom lakes would give accurate absorption values with the B2/B3 algorithm. This explains why the shallow lakes got a correlation but not a perfect correlation. Zhu et al (2014) found that the inclusion of longer wavelength bands (>600 nm) were effective to the performance of empirical models which could produce more successful results in a future study.

However, increased or varying effects of optical disturbances with depth could be a reason why the lakes classified as deep did not get any significant correlation. If the issue then was of

physical optic disturbances such as refraction and absorption (as pure water in itself absorbs longer wavelengths) the band ratio algorithm would be less effective or only applicable to lakes of the same depth. If the optical disturbances was with turbidity or particulate organic carbon (POC) the difference between the filtered water sample absorptions and what would be detected by a satellite could make the data unmatchable, although that scenario is quite unlikely for the clear waters in the subarctic lakes.

Another reason that the lakes classified as deep did not get the same correlation could be that there is not enough spread of absorption values for the lakes in the study. Thereby being unable to produce a fitting curve as the values available are too few and clustered in a too short range. Which also leads to speculations whether the fitted curves for 'deep' and 'shallow' might just be slightly offset for the overall results to give a significant correlation.

The conclusions drawn above is supported in the IOCCG (2000) publication but for stronger conclusions to be drawn more lakes and more data of the lakes characteristics would need to be analyzed.

### 4.5. Timing

In a DOC study by Olefeldt & Roulet (2011) of the same target lakes, they find that the snowmelt period affect annual DOC export from palsa and bog catchments differently than the fens. Thus since the snowmelt is considered to be responsible for more than half of the annual DOC export (Finlay et al., 2006), which started in early to mid-April in 2009 (Olefeldt & Roulet, 2011); the CDOM concentration for in situ sampling in May and image acquisitions from July and August might be more temporally impacted than initially expected. This should be kept in mind for future studies, where sampling could be done with respect to satellite fly-overs and clear skies. Characteristics data of the draining peatland-type to the specific lake could also be of interest. Especially since Cardille et al. (2013) have found a successful method for Canadian lakes in utilizing legacy lake samples and newer, high quality, satellite images. Their method is relying on knowledge of the in-lake CDOM processes and variations but eliminates the need for exactly timed images, which could be the most appropriate for this region.

### 4.6. Future studies

For future studies images from a higher radiometric and ground resolution sensor would be needed since the $a_{CDOM}$ values are low and the lakes are small and sensitive to optical disturbances. Other suitable sensors are:

- Enhanced Thematic Mapper (ETM), Landsat 7 satellite. Same ground resolution (30 m) and same band widths (7 + 1 bands, 0.45 – 2.35 μm) but with better radiometric resolution.
- Advanced Land Imager (ALI), EO-1 satellite. Same ground resolution (30 m) but with better band width resolutions (7 + 1 bands, 0.433 – 2.35 μm).
- Operational Land Imager (OLI), Landsat 8 satellite. Same ground resolution (30 m) but better band width resolutions (9 bands, 0.43 – 2.29 μm).
- Compact High Resolution Imaging Spectrometer (CHRIS), PROBA-1 satellite. Better ground resolution (18 m) and better band width resolutions (18 bands, 0.438 – 1.035 μm).

Out of the sensors listed the CHRIS from the European Space Agency looks the most suitable because of both having better ground- and band width resolutions. With increased ground resolution more lakes could also be included in the study which would be preferable for the smaller subarctic lakes in connection to fens, palsas, bogs and mires; it might even be able to include some streams, but more interestingly the shifts of DOC concentrations through the aquatic network in the catchment could be mapped where hotspots or sinks could be monitored. The shorter band width

resolutions would also make it possible to customize the algorithm very specifically. However the satellite has for the last decade had some issues; making reconstruction of past DOC concentrations improbable and only usable if in situ measurements are updated. Although the in situ measurements are still recommended to be updated and to include more information about the lakes as it would aid in drawing stronger conclusions about lake characteristics effect on CDOM absorption and correlation to remote sensed values which would in turn be used for optimizing the estimation algorithm. During in situ surveys specific radiances could also be measured and used in a more thorough atmospheric correction, which would be needed for all of the sensors listed above due to their higher sensitivity.

## 5. Conclusions

The Landsat TM-5 images are not generally suitable for estimating chromophoric dissolved organic matter in the Stordalen area. However it appears as if better results could be yielded if the satellite sensor used were of higher spectral or radiometric resolution and had better ground resolution for small lakes to be adequately represented, and if the in situ sample data was extended and included more information on lake characteristics; stronger conclusions could be drawn and corrected for in the choice of appropriate algorithm.

## 6. References


Berggren, M., H. Laudon, and M. Jansson (2009), Hydrological control of organic carbon support for bacterial growth in boreal headwater streams, Microb. Ecol., 57, 170–178, doi:10.1007/s00248-008-9423-6.

Cardille, J. A., Leguet, J. B., & del Giorgio, P. (2013). Remote sensing of lake CDOM using noncontemporaneous field data. *Canadian Journal of Remote Sensing*, *39*(02), 118-126.

Callaghan, T. V., Bergholm, F., Christensen, T. R., Jonasson, C., Kokfelt, U., & Johansson, M. (2010). A new climate era in the sub-Arctic: Accelerating climate changes and multiple impacts. *Geophysical Research Letters*, *37*(14), L14705.

Ekström, S. M., Kritzberg, E. S., Kleja, D. B., Larsson, N., Nilsson, P. A., Graneli, W., & Bergkvist, B. (2011). Effect of acid deposition on quantity and quality of dissolved organic matter in soil–water. *Environmental science & technology*, *45*(11), 4733-4739.

ESRI. 2014. ESRI Support, GIS Dictionary, Radiometric Resolution. [online] Available at: http://support.esri.com/en/knowledgebase/GISDictionary/term/radiometric%20resolution [Accessed 2014-01-07]

Exelis VIS. 2014. Fast Line-of-sight Atmospheric Analysis of Hypercubes (FLAASH). [online] Available at: http://www.exelisvis.com/docs/FLAASH.html [Accessed: 2013-10-02]

Finlay, J., J. Neff, S. Zimov, A. Davydova, and S. Davydov (2006), Snowmelt dominance of dissolved organic carbon in high-latitude watersheds: Implications for characterization and flux of river DOC, Geophys. Res. Lett., 33, L10401, doi:10.1029/2006GL025754.

Finlay, K., Leavitt, P. R., Wissel, B., & Prairie, Y. T. (2009). Regulation of spatial and temporal variability of carbon flux in six hard-water lakes of the northern Great Plains. *Limnology and Oceanography*, *54*(6), 2553.

Griffin, C. G., Frey, K. E., Rogan, J., & Holmes, R. M. (2011). Spatial and interannual variability of dissolved organic matter in the Kolyma River, East Siberia, observed using satellite imagery. *Journal of Geophysical Research*,*116*(G3), G03018.

Hirtle, H., & Rencz, A. (2003). The relation between spectral reflectance and dissolved organic carbon in lake water: Kejimkujik National Park, Nova Scotia, Canada. *International Journal of Remote Sensing*, *24*(5), 953-967.

INTERGOVERNMENTAL PANEL ON CLIMATE CHANGE (IPCC). (2007). Solomon, S., D. Qin, M. Manning, Z. Chen, M. Marquis, K. B. Averyt, M. Tignor and H. L. Miller [eds.], Climate change 2007: The physical science basis. Contribution of Working Group I to the Fourth Assessment Report of the Intergovernmental Panel on Climate Change. Cambridge Univ. Press.

IOCCG (2000). Remote Sensing of Ocean Colour in Coastal, and Other Optically-Complex, Waters. Sathyendranath, S. (ed.), Reports of the International Ocean-Colour Coordinating Group, No. 3, IOCCG, Dartmouth, Canada

Jansson, M., Hickler, T., Jonsson, A., & Karlsson, J. (2008). Links between terrestrial primary production and bacterial production and respiration in lakes in a climate gradient in subarctic Sweden. *Ecosystems*, *11*(3), 367-376.

Johansson, M., Åkerman, J., Keuper, F., Christensen, T. R., Lantuit, H., & Callaghan, T. V. (2011). Past and

present permafrost temperatures in the Abisko area: Redrilling of boreholes. *Ambio, 40*(6), 558-565.

Kallio, K., Attila, J., Härmä, P., Koponen, S., Pulliainen, J., Hyytiäinen, U-M., Pyhälahti, T. (2008). Landsat ETM+ Images in the estimation of seasonal lake water quality in boreal river basins. Environmental Management, 42:511-522, DOI 10,1007/s00267-008-9146-y.

Kullman, L. (2002). Rapid recent range- margin rise of tree and shrub species in the Swedish Scandes. *Journal of ecology*, *90*(1), 68-77.

Kutser, T., Pierson, D., Reinart, A., Sobek, S., Kallio, K. (2004). Mapping lake CDOM by satellite remote sensing. *Remote Sensing of Environment*, 94, 4, p 535-540.

Kutser, T., Pierson, D., Tranvik, L. (2005). Using Satellite Remote Sensing to Estimate the Coloured Dissolved Organic Matter Absorption Coefficient in Lakes. *Ecosystems (2005)* 8: 709-720. DOI: 10.1007/s10021-003-0148-6.

Kutser, T. (2012). The possibility of using the Landsat image archive for monitoring long time trends in coloured dissolved organic matter concentration in lake waters. *Remote Sensing of Environment*, *123*, 334-338.

Lapierre, J. F., Guillemette, F., Berggren, M., & del Giorgio, P. A. (2013). Increases in terrestrially derived carbon stimulate organic carbon processing and CO2 emissions in boreal aquatic ecosystems. *Nature communications*, *4*.

Laudon, H., Buttle, J., Carey, S. K., McDonnell, J., McGuire, K., Seibert, J., ... & Tetzlaff, D. (2012). Cross- regional prediction of long- term trajectory of stream water DOC response to climate change. *Geophysical Research Letters*, *39*(18).

Malmer, N., T. Johansson, M. Olsrud, and T.R. Christensen. 2005. Vegetation, climatic changes and net carbon sequestration in a North-Scandinavian subarctic mire over 30 years. *Global Change Biology 11:* 1895-1909.

Miller. R. L., Del Castillo. C. E., McKee. B. A., 2005. Remote sensing of coastal aquatic environments – Technologies, Techniques and Applications. Volume 7. Remote sensing of organic matter in coastal waters. Chapter 7. ISBN 1-4020-3100-9. Springer, Dordrecht, The Netherlands.

Monteith, D. T., Stoddard, J. L., Evans, C. D., de Wit, H. A., Forsius, M., Høgåsen, T., ... & Vesely, J. (2007). Dissolved organic carbon trends resulting from changes in atmospheric deposition chemistry. *Nature*, *450*(7169), 537-540.

Olefeldt, D., & Roulet, N. T. (2012). Effects of permafrost and hydrology on the composition and transport of dissolved organic carbon in a subarctic peatland complex. *Journal of Geophysical Research: Biogeosciences (2005–2012)*,*117*(G1).

Olmanson, L. G., Bauer, M. E., & Brezonik, P. L. (2008). A 20-year Landsat water clarity census of Minnesota's 10 000 lakes. Remote Sensing of Environment, 112, 4086–4097

Olmanson, L. G., Brezonik, P. L., & Bauer, M. E. (2011). Evaluation of medium to low resolution satellite imagery for regional lake water quality assessments. Water Resources Research, 47, http://dx.doi.org/10.1029/WR011005.

Regnier, P., Friedlingstein, P., Ciais, P., Mackenzie, F. T., Gruber, N., Janssens, I. A., ... & Thullner, M. (2013). Anthropogenic perturbation of the carbon fluxes from land to ocean. *Nature Geoscience*.

Roulet, N., & Moore, T. R. (2006). Environmental chemistry: Browning the waters. *Nature*, *444*(7117), 283-284.

Romanovsky, V.E., S.L. Smith, & H.H. Christiansen. (2010). Permafrost thermal state in the polar Northern Hemisphere during the international polar year 2007–2009: A synthesis. *Permafrost and Periglacial Processes* 21: 106–116.

Smith, G. M., & Milton, E. J. (1999). The use of the empirical line method to calibrate remotely sensed data to reflectance. *International Journal of Remote Sensing*, *20*(13), 2653-2662.

Spectral Sciences Incorporated. 2012. Modtran5. [online] Available at: http://www.modtran5.com/ [Accessed: 2014-01-20]

Tanré, D., Deschamps, P. Y., Duhaut, P., & Herman, M. (1987). Adjacency effect produced by the atmospheric scattering in thematic mapper data. *Journal of Geophysical Research: Atmospheres (1984–2012)*, *92*(D10), 12000-12006.

Tarnocai, C., Canadell, J. G., Schuur, E. A. G., Kuhry, P., Mazhitova, G., & Zimov, S. (2009). Soil organic carbon pools in the northern circumpolar permafrost region. *Global biogeochemical cycles*, *23*(2).

Tranvik, L. (1996). Photo-oxidative production of dissolved inorganic carbon in lakes of different humic content. *Limnol. Oceanogr*, *41*(4), 698-706.

Tranvik, L. J., Downing, J. A., Cotner, J. B., Loiselle, S. A., Striegl, R. G., Ballatore, T. J., ... & Weyhenmeyer, G. A. (2009). Lakes and reservoirs as regulators of carbon cycling and climate. *Limnology and Oceanography*, *54*(6), 2298-2314.

USGS Landsat Missions. 2013a. Landsat 5 History. [online] Available at: https://landsat.usgs.gov/about_landsat5.php [Accessed: 2013-12-20]

USGS Landsat Missions. 2013b. Landsat 4-5 Thematic Mapper (TM) Calibration Notices. [online] Available at: https://landsat.usgs.gov/science_L4-5_Cal_Notices.php [Accessed: 2013-12-20]

Zhu, W., Yu, Q., Tian, Y. Q., Becker, B. L., Zheng, T., & Carrick, H. J. (2014). An assessment of remote sensing algorithms for colored dissolved organic matter in complex freshwater environments. *Remote Sensing of Environment*,*140*, 766-778.

Institutionen för naturgeografi och ekosystemvetenskap, Lunds Universitet.

**Student examensarbete (Seminarieuppsatser). Uppsatserna finns tillgängliga på institutionens geobibliotek, Sölvegatan 12, 223 62 LUND. Serien startade 1985. Hela listan och själva uppsatserna är även tillgängliga på LUP student papers (www.nateko.lu.se/masterthesis) och via Geobiblioteket (www.geobib.lu.se)**

The student thesis reports are available at the Geo-Library, Department of Physical Geography and Ecosystem Science, University of Lund, Sölvegatan 12, S-223 62 Lund, Sweden. Report series started 1985. The complete list and electronic versions are also electronic available at the LUP student papers (www.nateko.lu.se/masterthesis) and through the Geo-library (www.geobib.lu.se)

245 Linnea Jonsson (2012). Impacts of climate change on Pedunculate oak and Phytophthora activity in north and central Europe

246 Ulrika Belsing (2012) Arktis och Antarktis föränderliga havsistäcken

247 ***Anna Lindstein (2012) Riskområden för erosion och näringsläckage i Segeåns avrinningsområde***

248 Bodil Englund (2012) Klimatanpassningsarbete kring stigande havsnivåer i Kalmar läns kustkommuner

249 Alexandra Dicander (2012) GIS-baserad översvämningskartering i Segeåns avrinningsområde

250 Johannes Jonsson (2012) Defining phenology events with digital repeat photography

251 Joel Lilljebjörn (2012) Flygbildsbaserad skyddszonsinventering vid Segeå

252 Camilla Persson (2012) Beräkning av glaciärers massbalans – En metodanalys med fjärranalys och jämviktslinjehöjd över Storglaciären

253 Rebecka Nilsson (2012) Torkan i Australien 2002-2010 Analys av möjliga orsaker och effekter

254 Ning Zhang (2012) Automated plane detection and extraction from airborne laser scanning data of dense urban areas

255 Bawar Tahir (2012) Comparison of the water balance of two forest stands using the BROOK90 model

256 Shubhangi Lamba (2012) Estimating contemporary methane emissions from tropical wetlands using multiple modelling approaches

257 Mohammed S. Alwesabi (2012) MODIS NDVI satellite data for assessing drought in Somalia during the period 2000-2011

258 Christine Walsh (2012) Aerosol light absorption measurement techniques: A comparison of methods from field data and laboratory experimentation

259 Jole Forsmoo (2012) Desertification in China, causes and preventive actions in modern time

260 Min Wang (2012) Seasonal and inter-annual variability of soil respiration at Skyttorp, a Swedish boreal forest

261 Erica Perming (2012) Nitrogen Footprint vs. Life Cycle Impact Assessment methods – A comparison of the methods in a case study.

262 Sarah Loudin (2012) The response of European forests to the change in summer temperatures: a comparison between normal and warm years, from

1996 to 2006

263 Peng Wang (2012) Web-based public participation GIS application – a case study on flood emergency management

264 Minyi Pan (2012) Uncertainty and Sensitivity Analysis in Soil Strata Model Generation for Ground Settlement Risk Evaluation

265 Mohamed Ahmed (2012) Significance of soil moisture on vegetation greenness in the African Sahel from 1982 to 2008

266 Iurii Shendryk (2013) Integration of LiDAR data and satellite imagery for biomass estimation in conifer-dominated forest

267 Kristian Morin (2013) Mapping moth induced birch forest damage in northern Sweden, with MODIS satellite data

268 Ylva Persson (2013) Refining fuel loads in LPJ-GUESS-SPITFIRE for wet-dry areas - with an emphasis on Kruger National Park in South Africa

269 Md. Ahsan Mozaffar (2013) Biogenic volatile organic compound emissions from Willow trees

270 Lingrui Qi (2013) Urban land expansion model based on SLEUTH, a case study in Dongguan City, China

271 Hasan Mohammed Hameed (2013) Water harvesting in Erbil Governorate, Kurdistan region, Iraq - Detection of suitable sites by using Geographic Information System and Remote Sensing

272 Fredrik Alström (2013) Effekter av en havsnivåhöjning kring Falsterbohalvön.

273 Lovisa Dahlquist (2013) Miljöeffekter av jordbruksinvesteringar i Etiopien

274 Sebastian Andersson Hylander (2013) Ekosystemtjänster i svenska agroforestrysystem

275 Vlad Pirvulescu (2013) Application of the eddy-covariance method under the canopy at a boreal forest site in central Sweden

276 Malin Broberg (2013) Emissions of biogenic volatile organic compounds in a Salix biofuel plantation – field study in Grästorp (Sweden)

277 Linn Renström (2013) Flygbildsbaserad förändringsstudie inom skyddszoner längs vattendrag

278 Josefin Methi Sundell (2013) Skötseleffekter av miljöersättningen för natur- och kulturmiljöer i odlingslandskapets småbiotoper

279 Kristín Agustsdottír (2013) Fishing from Space: Mackerel fishing in Icelandic waters and correlation with satellite variables

280 Cristián Escobar Avaria (2013) Simulating current regional pattern and composition of Chilean native forests using a dynamic ecosystem model

281 Martin Nilsson (2013) Comparison of MODIS-Algorithms for Estimating Gross Primary Production from Satellite Data in semi-arid Africa

282 Victor Strevens Bolmgren (2013) The Road to Happiness – A Spatial Study of Accessibility and Well-Being in Hambantota, Sri Lanka

283 Amelie Lindgren (2013) Spatiotemporal variations of net methane emissions and its causes across an ombrotrophic peatland - A site study from Southern Sweden

284 Elisabeth Vogel (2013) The temporal and spatial variability of soil respiration in boreal forests - A case study of Norunda forest, Central Sweden

285 Cansu Karsili (2013) Calculation of past and present water availability in the Mediterranean region and future estimates according to the Thornthwaite water-balance model

286 Elise Palm (2013) Finding a method for simplified biomass measurements on Sahelian grasslands

287 Manon Marcon (2013) Analysis of biodiversity spatial patterns across multiple taxa, in Sweden
288 Emma Li Johansson (2013) A multi-scale analysis of biofuel-related land acquisitions in Tanzania - with focus on Sweden as an investor
289 Dipa Paul Chowdhury (2013) Centennial and Millennial climate-carbon cycle feedback analysis for future anthropogenic climate change
290 Zhiyong Qi (2013) Geovisualization using HTML5 - A case study to improve animations of historical geographic data
291 Boyi Jiang (2013) GIS-based time series study of soil erosion risk using the Revised Universal Soil Loss Equation (RUSLE) model in a micro-catchment on Mount Elgon, Uganda
292 Sabina Berntsson & Josefin Winberg (2013) The influence of water availability on land cover and tree functionality in a small-holder farming system. A minor field study in Trans Nzoia County, NW Kenya
293 Camilla Blixt (2013) Vattenkvalitet - En fältstudie av skånska Säbybäcken
294 Mattias Spångmyr (2014) Development of an Open-Source Mobile Application for Emergency Data Collection
295 Hammad Javid (2013) Snowmelt and Runoff Assessment of Talas River Basin Using Remote Sensing Approach
296 Kirstine Skov (2014) Spatiotemporal variability in methane emission from an Arctic fen over a growing season – dynamics and driving factors
297 Sandra Persson (2014) Estimating leaf area index from satellite data in deciduous forests of southern Sweden
298 Ludvig Forslund (2014) Using digital repeat photography for monitoring the regrowth of a clear-cut area
299 Julia Jacobsson (2014) The Suitability of Using Landsat TM-5 Images for Estimating Chromophoric Dissolved Organic Matter in Subarctic Lakes
300 Johan Westin (2014) Remote sensing of deforestation along the trans-Amazonian highway